EFFECT OF EDGE DISLOCATIONS ON ATOMIC DIFFUSION IN A SUPERALLOY WITH THERMAL BARRIER COATING

Bárbara González Rolón[1] and Sandra Eloisa Chávez Alfaro[2]

[1,2] Department of Mechanical Engineering, Universidad de Guanajuato, Carretera Salamanca-Valle de Santiago Km. 3.5+ 1.8; Comunidad de Palo Blanco, Salamanca, Guanajuato, 36885, MÉXICO.
Authors Email: barbara@ugto.mx[1] and sandra.echavez@hotmail.com[2]

Published: 27 December 2019

Abstract

In this investigation, the diffusion coefficient for nickel was determined, considering the effect of edge dislocations present in the substrate of a UDIMET 500 superalloy closet to the thermal barrier of ZrO_2 -Y_2O_3 as a coating, of a failed blade of a turbine of gas for the generation of electric power. The blade was in operation at a temperature of 1050°C, with a useful life of approximately 30,000 h. The analysis of the dislocations was made with an SEM QUANTA 3D 200, and the determination of the effective diffusion coefficient Deff for the Ni was obtained from the Smoluchowski model and the Hart equations. With the modeling of Smoluchowski dislocation tubes and the solutions of Le Claire and Rabinovitch, the graphic representation of the diffusion coefficient was obtained, which is a function of the average logarithmic concentration <c> against the square of the distance perpendicular to the fault zone, from which the value obtained for the effective diffusion coefficient is, 3.08E-11 cm^2/s

Keywords: Edge dislocations; diffusion coefficient; superalloy; thermal barrier

Cite this article: Rolón, B.G. & Alfaro, S.E.C. (2019). Effect Of Edge Dislocations On Atomic Diffusion In A Superalloy With Thermal Barrier Coating. *European International Journal of Science and Technology*, 8(11), 50-63.

INTRODUCTION

Nowadays, the continuous evolution of materials for high temperatures, the development, and analysis of coatings for gas turbines is being a decisive factor in the progression of equipment for power generation, and other applications. This research analyzes the behavior of atomic diffusion of the Ni towards the coating in the presence of linear dislocations. In the substrate, by the fault in a gas turbine of the first step with approximately 30,000h of service, which will allow knowing if its presence influences in the accelerated atomic migration that occurs in this section of the material and its failure.

With the modeling of Smoluchowski dislocation tubes and the solutions of Le Claire and Rabinovitch [1], the graphic representation of the diffusion coefficient was obtained, which is a function of the average logarithmic concentration <c> against the square of the distance perpendicular to the fault zone y^2, from which the next expression is obtained for the effective diffusion coefficient Deff .

$$D_{eff} = (4t \frac{\partial \ln <c>}{\partial y^2})^{-1} \qquad (1)$$

Hart equations [2]. They will be used to calculate the unique coefficient of the superalloy sample. The model and the experimental parameters found for the calculations are briefly described below.

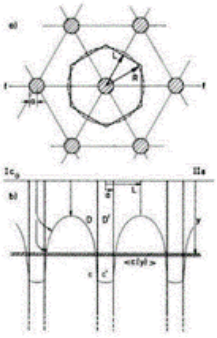

Fig. 1 (a) Plan view of a hexagonal array of dislocation pipes; pipe radius a, spacing 2L. Bold lines: Wigner-Seitz-type cell, a hexagonal prism; broken lines: the equivalent circular cylinder of same cross-sectional area, radius R. (b) Vertical section through f-f of fig.1(a), showing the trace of a contour of constant concentration; <c(y)> is the average concentration in the section, shown hatched, at depth y.[1]

Smoluchowski considered a cylindrical tube of radius a within which homogeneous and isotropic diffusion occurs. Fick first law with the diffusion coefficient due to the defects D ', which is considered much higher than the coefficient of D diffusion in a monocrystal, far from the radius of dislocation at the radial distance, from the heart 2.68E-11t of the dislocation fig.1(b). The model considers the influence of dislocations in the diffusion, from a surface y=0 contained in a semi-infinite solid. Another important consideration is in the arrangement of dislocations, which are parallel to each other and perpendicular to the studied surface, where there are, dislocations per unit area.

The diffusion occurs from the surface with diffusion coefficient D outside the tubes. But there is rapid diffusion in the material at a rate determined by the coefficient D '. Those produce losses at the edges governed in the same way by D. The equations of the model where c and c' respectively represent the diffuse concentrations outside, and inside the dislocation tube respectively, R is the radius of the Wigner-Seitz cylinder, which is equal to the average distance between dislocations fig.1(a)

Inside the dislocation tube (0≤ r ≤a) you have:

$$D\left\{\frac{1}{r}\frac{\partial}{\partial r}\left(r\frac{\partial c}{\partial r}\right)+\frac{\partial^2 c}{\partial y^2}\right\}=\frac{\partial c}{\partial t} \quad (2)$$

Outside the dislocation tube (a≤ $r \leq R$):

$$D'\left\{\frac{1}{r}\frac{\partial}{\partial r}\left(r\frac{\partial c'}{\partial r}\right)+\frac{\partial^2 c'}{\partial y^2}\right\}=\frac{\partial c'}{\partial t} \quad (3)$$

From the model and other contributions, we obtain the two first cases for the solution of the model and its empirical equation for the calculation of the dislocation density:

The case I: The concentration on the surface of the material remains constant (Co) at a time time t≥ 0. The case I, is appropriate for diffusion within a sample that is in a vapor phase Co, is the equilibrium concentration of the vapor, at the surface of the material. From this consideration, we have the following experimental equation to obtain the density of dislocations [1] d^I.

$$d^I=\frac{\left(\langle c\rangle^I_{Int}/_{c_o}\right)}{\pi a^{0.16}(Dt)^{0.92}} \quad (4)$$

Case II: There is a thin diffuse layer in a quantity γ per unit area, which was deposited at time t = 0. Similarly, case II also has its expression for the density of dislocations [1] d^{II}.

$$d^{II}=\frac{\left[\langle c\rangle^{II}_{Int}/_{c_o}\right]}{\pi^{3/2}a^{0.16}(Dt)^{1.42}(\partial \ln\langle c\rangle/\partial y)_{Tail}} \quad (5)$$

Effective diffusion coefficient calculation.

Case II attempts to simulate the general conditions of a thin layer by plotting its diffusion measurement. However, it is very appropriate if in practice there is no rapid diffusion along the surface through the dislocations to compensate for the loss near r = 0 due to the rapid diffusion below them. On the other hand, the case I, it may be in practice more appropriate if only a minimal layer deposited and diffused in the sample, for example, when there is only small solubility or diffusion, also applies when the diffusion time is very short, or the temperature is low. While the concentrations calculated on I or II differ, the gradient $\partial \log < c > /\partial y$, of the dislocation tails are equal in both cases; this characteristic is influenced by the uncertainty that can be presented by the surface conditions. Finally, after analyzing the parameters obtained, the appropriate approximation was searched for the calculation of the effective diffusion coefficient and was found by the expression of Hart.[2]

$$D_{eff} \rightarrow D_{Hart}=\varepsilon^2 D'+(1-\varepsilon^2)D \quad (6)$$

$$D_{Hart}=D(1+\varepsilon^2(\Delta-1)) \quad (7)$$

Where the volume fraction of the material in the dislocation is ε^2, and the relationship between the diffusion coefficient due to the defects and that of the crystal diffusion coefficient is Δ.

$$\varepsilon^2=\pi a^2 d \quad (8)$$

$$\Delta=\frac{D'}{D} \quad (9)$$

EXPERIMENTAL SET UP AND METHODOLOGY

Analysis of the substrate.

From a failed blade of the first-pass gas turbine, of the section that had high heating, a sample was cut with the substrate and thermal barrier, this sample was prepared and subsequently polished with a column of gallium ions in the Quanta Electronic Scanning Microscope 3D 200. After that, a chemical and metallographic analysis was carried out, by stereoscopic and electronic scanning microscopy. From this analysis comparing with the chemical composition of the UDIMET 500 18wt%Cr, 18.5wt%Co, 4.0wt%Mo, 2.9wt% Al, 2.9wt%Ti, 0.08wt%C, 0.006wt%B, 0.05wt%Zr [3]. The substrate was considered to correspond to the UDIMET 500 superalloy. The failed blade of a turbine of gas was in operation at a temperature of 1050°C, with a useful life of approximately 30,000h. The chemical composition of the substrate was determined with a Perkin Elmer ICP spectrophotometer, the determination of carbon and sulfur was in a LECO CS230. The substrate was found to be formed by fine particles γ' of the first range, in a matrix γ and M23C6 carbides precipitated in the grain boundaries fig.2

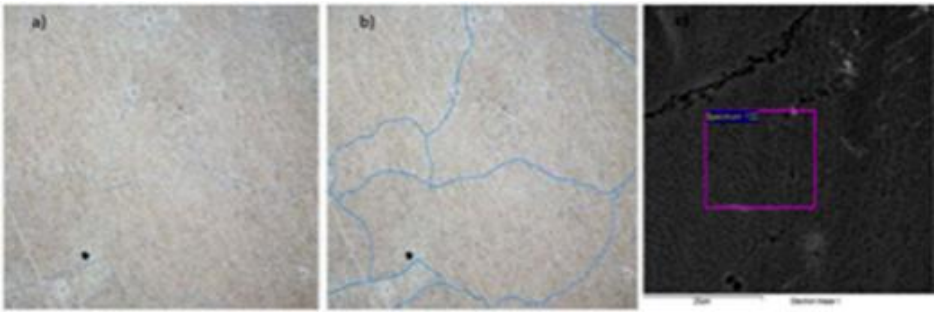

Fig.2 Microstructure of the sample (a) Grain boundaries where the $M_{23}C_6$ is located (b) Detail of grain boundaries made by CAD. (c) Fine particles of γ ' a in matrix γ.

From the study sample, a 999X micrograph was taken, with the QUANTA 3D 200 electronic scanning microscope, fig.3

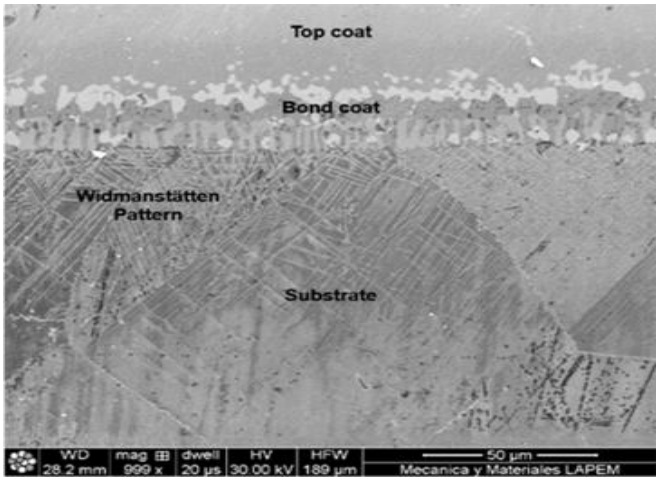

Fig. 3 The UDIMET 500 substrate micrograph 999x.

The thermal barrier coating of this substrate consists of two layers: a "Top Coat" with a low thermal conductivity of ZrO_2-Y_2O_3. Which may contain small additions of elements such as Pt, Hf, Ta and the "Bond Coat," is an oxidation-resistant intermetallic layer also known as an adhesive layer, this layer is generally composed of diffusion aluminide or platinum aluminide or an overlay of NiCoCrAlY composition, according to the formation of the substrate [7]. Fig.3

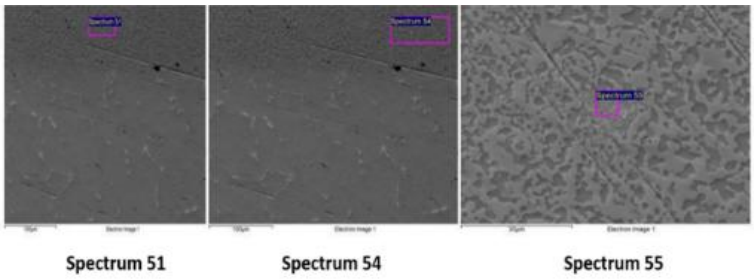

Fig.4 Micrograph obtained after of energy dispersion analysis by spectroscopy in the bond coat section, the inspection area is inside the rectangle.

With dispersed energy spectroscopy, the chemical composition of the Bond Coat of the UDIMET 500 superalloy was analyzed, table 1, fig. 4

Tabla 1. Chemical composition of Bond Coat

Area	Al w/o	Cr w/o	Co w/o	Ni w/o	Ti w/o	Y w/o
29	9.89	20.32	34.36	35.44	---	---
42	10.24	20.12	33.50	36.14	---	---
46	11.01	7.58	16.73	33.76	0.21	30.71

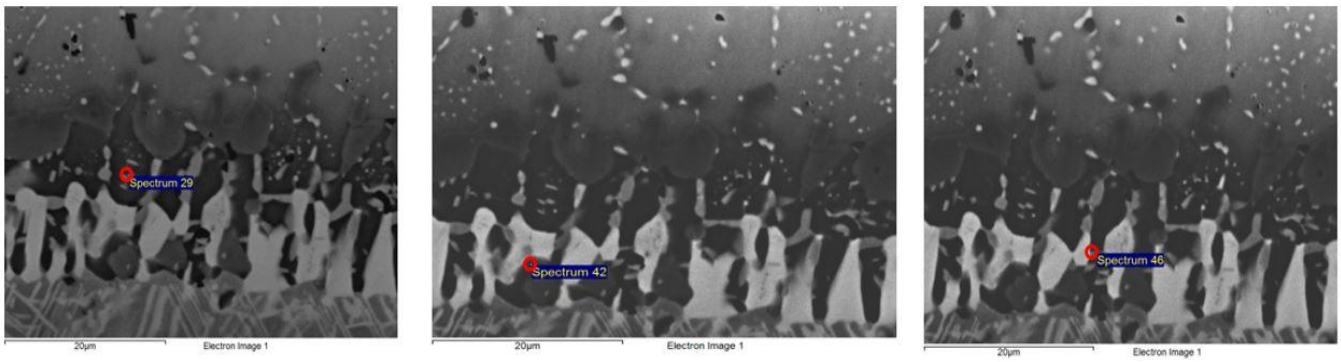

Fig. 5 Analysis of Chemical composition in specific areas of the sample in the bond coat

From the analysis of composition table 1, and the point analysis of composition for the bond coat in the area closest to the substrate table 2. It was observed that the chemical composition next to the substrate presents essential variations for chromium, nickel and of minor importance for aluminum, in addition to the appearance of iron and molybdenum titanium, which belong to the substrate, which indicates a migration of chemical elements from the substrate to the bond coat.

Table 2. Elements present in the Bond Coat of the region closest to the substrate.

Test	Al w/o	Ti w/o	Cr w/o	Co w/o	Ni w/o	Mo w/o	Pt w/o	Fe w/o	Zr w/o
1	1.39	1.44	37.4	24.58	16.85	17.92	*	0.42	*
2	16.73	2.63	10.88	16.76	46.69	4.17	*	0.42	1.72
3	19.36	3.1	6.28	16.44	53.13	*	1.38	0.31	*
4	10.92	3.91	14.28	17.49	46.37	5.57	1.45	*	*
5	1.76	0.85	41.4	25.88	11.16	18.33	*	0.62	*
6	1.13	0.81	42.82	25.33	11.68	17.71	*	0.52	*
7	2.96	0.86	39.13	24.91	15.17	16.46	*	0.51	*

Analysis of linear defects

Dislocations in a micrograph are presented as corrosion patterns [4]. Fig. 6 shows a sample section taken from fig.3 in which, using the CAD Software, the lengths of each of the dislocations found were identified and measured. This data allowed us to calculate the density of the dislocation per unit of area d^{II}

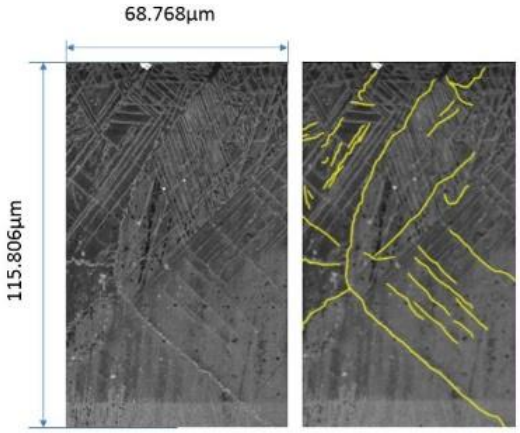

Fig 6. Location of dislocations in a section of the sample analyzed.

From fig.6, the total length of the dislocations identified in an area of $A = 7.96402x10^{-9}m^2$ and a length of $l_d = 0.00057716m$

Calculation of the depth of electromagnetic radiation.

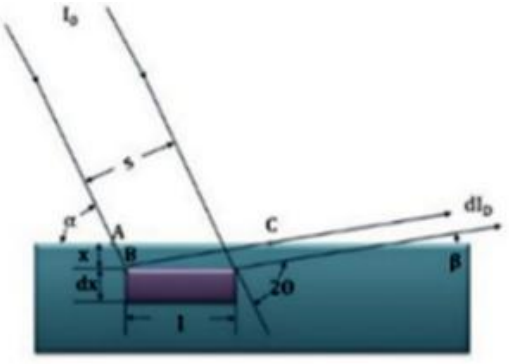

Fig 7. Model for dispersion analysis [5].

From the geometry present in fig.7. It was found the equation (10) for the energy flow per second of a beam diffracted outside the specimen, and then below is the development to obtain the finite thickness [5].

$$dI_D = abI_o e^{-\mu(AB+BC)}dx \qquad (10)$$

From the geometry of fig 7 we obtain:

$$l = \frac{s}{\sin\alpha'} \quad AB = \frac{x}{\sin\alpha'} \quad BC = \frac{x}{\sin\beta} \qquad (11)$$

From the previous expressions start with the equation:

$$dI_D = \frac{I_o sab}{\sin\alpha} e^{-\mu x(\frac{1}{\sin\alpha}+\frac{1}{\sin\beta})}dx \qquad (12)$$

From where:

I_o: The intensity of the incident ray (erg /cm^{2}s)

dI_D: Energy flow per second (erg/s)

s: Thickness

α: Incident angle

β: Diffraction angle

θ: Dispersion angle

l: The plane length that diffracts energy

x: Depth below the surface

dx: Thickness

a: The volume fraction of the specimen containing the orientation to diffract the incident ray

b: The fraction of incident energy that is diffracted per unit volume

μ: Linear absorption coefficient.

The use of a flat specimen makes the incident and diffracted rays equal, and also causes to absorption coefficient to be independent of the angle θ: For this particular arrangement of the sample used in the diffractometer $\alpha = \beta = \theta$ and equation (12), it becomes:

$$dI_D = \frac{I_o sab}{sen\alpha} e^{(\frac{-2\mu x}{sen\Theta})}dx \qquad (13)$$

After obtaining equation (12) and adopting the criterion of infinite thickness, which depends on the sensitivity of the intensity measurements, or in what we call negligible diffracted intensity. In which the infinite depth "t" can be defined arbitrarily and reasonably through the intensity diffracted by the back layer it must be of 1/1000 the intensity diffracted by the upper part approximately [5], which allows us to write the equations (14) (15)

$$\frac{dI_D\,(ax=0)}{dI_D(ax=t)} = e^{\left(\frac{2\mu x}{\sin\theta}\right)} = 1000 \quad (14) \qquad \text{So "}t\text{":} \qquad t = \frac{3.45\ \sin\theta}{\mu} \quad (15)$$

Calculation of the linear absorption coefficient.

The following equation (16) obtains the calculating of the linear absorption coefficient [5].

$$\frac{\mu}{\rho} = \omega_1\left(\frac{\mu}{\rho}\right)_1 + \omega_2\left(\frac{\mu}{\rho}\right)_2 + \omega_3\left(\frac{\mu}{\rho}\right)_3 + \ldots \quad (16)$$

Table 3. Presents the mass-based absorption coefficients and the densities of the materials that make up the UDIMET 500.

Table 3. Absorption coefficients base mass for the elements of the UDIMET 500 [5]

Element	w/o	μ/ρ (cm^2/g)	ρ (g/cm^3)
Ni	52	49.3	8.90
Cr	19.3	259	7.19
Co	17.7	354	8.9
Mo	4.1	164	10.2
Al	3.4	48.7	2.70
Ti	3.1	204	4.54
Fe	0.3	324	7.87
Ca	0.07	172	1.55
Mn	0.001	284	7.43
Si	0.01	60.3	2.33
W	0.03	171	19.3

Using the equation (16) and the density of the UDIMET 500, the linear absorption coefficient of the sample is obtained $\mu = 154.13737\ cm^{-1}$.

Calculation of the dispersion angle.

With the Bragg's Law (17), we find the scattering angle (Θ)

$$\lambda = \frac{2a\ \sin\theta}{\sqrt{h^2+k^2+l^2}} \quad (17)$$

The target of the spectroscope used is Cu (the principal diffraction planes of Cu have the Miller Indexes all even or all odd), the zero is considered even. Thus the diffraction planes are: {111}, {200} and {220} the copper network constant is 3.6151x 10^{-10} m with power for the electron beam λ = 4.12958x10^{-11}m, with this data equation (17) was applied and found the dispersion angles and thicknesses table 4.

Table 4. Dispersion angles and layer thickness, for copper scattering planes.

Scatter plane	Dispersion angle	Thickness of layer (t) $x10^{-4}$ cm
{111}	5.6773°	2.485
{200}	6.5592°	2.870
{220}	9.2967°	4.057

With the data of table 4, an average thickness of 0.0003137 cm was obtained, with this data the density of the dislocation per unit volume was calculated $d^{II} = 2.31x10^{6} cm^{-2}$

Finally, the variation of the Ni chemical composition to the coating was determined in six lines on the zone where it was calculated the dislocation density with different trajectories perpendicular to the coating as shown in fig.7 and fig. 8, the path was sectioned into twenty points to obtain the percentage by weight at each position using spectroscopy in the SEM.

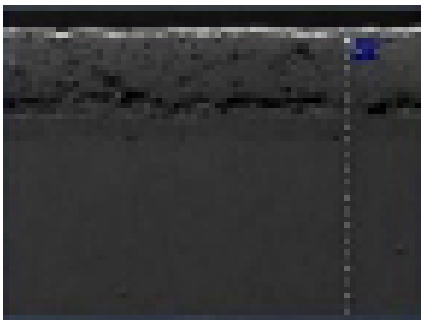

Fig. 7 Chemical analysis composition by SEM spectroscopy, on a line of 20 S(x) points on the substrate.

From this analysis, the composition curves of zone fig.8.

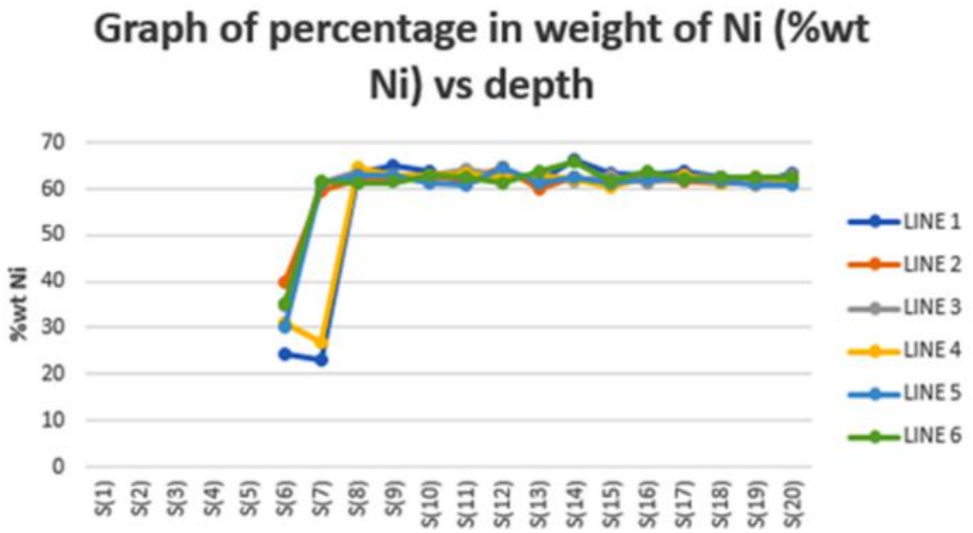

Fig.8 Graph of percentage by weight of nickel in the zone of the dislocations. The total depth analyzed was 15 µm.

From the graphs of percentage in weight of Ni versus the depth, it was obtained the lines of $ln\langle c\rangle\ vsy$ and is presented in figure 9.

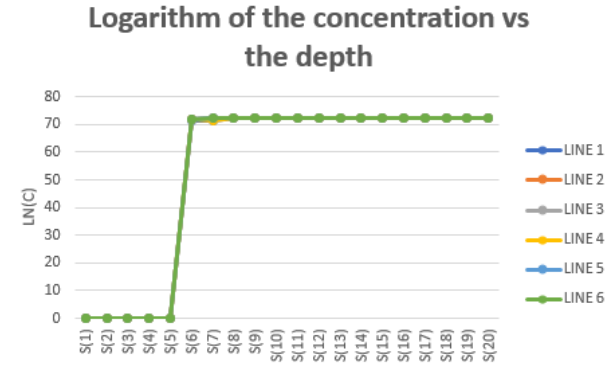

(a)

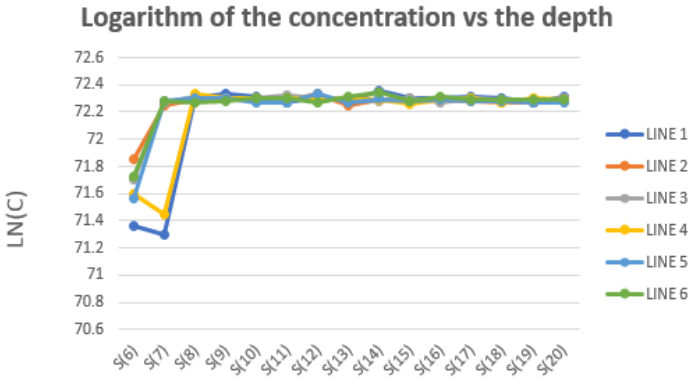

(b)

Fig. 9 a) Logarithm of concentration as a function of depth for the zone of dislocations, b) points for the regression.

From the graph (a) in the figure 9, the first five points in which there is no presence of Ni are discarded, and regression by least squares is performed, which gives the linear expression of the composition as a function of the depth, in turn, the initial composition and Co which is the composition of the first point where Ni appears. The results of the regressions of lines are presented in table 5.

Table 5. Regressions of the lines in the zone of dislocations (R, Data correlation coefficient)

Equation		R	$\partial \ln\langle c\rangle/\partial y$	$\langle c\rangle_{Int}^{II}$ (Atm/cm^3)	C_O (Atm/cm^3)
Line 1	$Ln\langle c\rangle = 71.821 + 0.0443y$	0.5759	0.0443	1.5541E+31	9.79E+30
Line 2	$Ln\langle c\rangle = 72.165 + 0.0111y$	0.4361	0.0111	2.1921E+31	1.60E+31
Line 3	$Ln\langle c\rangle = 72.143 + 0.0141y$	0.4133	0.0141	2.1444E+31	1.39E+31
Line 4	$Ln\langle c\rangle = 71.918 + 0.0342y$	0.5580	0.0342	1.7123E+31	1.24E+31
Line 5	$Ln\langle c\rangle = 72.101 + 0.0169y$	0.4062	0.0169	2.0562E+31	1.20E+31
Line 6	$Ln\langle c\rangle = 72.133 + 0.0154y$	0.4631	0.0154	2.1231E+31	1.41E+31

Calculation of the effective diffusion coefficient.

From the equation (18) the remaining parameters are calculated to obtain the calculation of the diffusion coefficient in the substrate for the elements that make up the alloy.

$$d^{II} = \frac{[\langle c \rangle_{Int}^{II} / c(0)]}{\pi^{3/2} a^{0.16} (Dt)^{1.42} (\partial \ln \langle c \rangle / \partial y)_{Tail}} \quad (18)$$

The following are the fixed and constant parameters that will be used in the calculation:
Dislocation density per unit volume d^{II}= 2.31x10^{6} cm $^{-2}$
Operating time t = 30000 h

The radius of the dislocation tube $a = 5x10^{-8} cm$ and A (α) The parameter that describes the slopes of the tails.

Table 6. D coefficient of diffusion for a perfect crystal and parameters for finding the linear domain.

	D (cm2/s)	E	α	ε/α
Line 1	1.0E-14	0.000135	4.80E-05	2.80
Line 2	2.34E-14	0.000135	3.14E-05	4.28
Line 3	2.16E-14	0.000135	3.27E-05	4.12
Line 4	1.08E-14	0.000135	4.62E-05	2.91
Line 5	2.04E-14	0.000135	3.37E-05	4.00
Line 6	1.99E-14	0.000135	3.41E-05	3.95

$$\frac{\partial \ln\langle c\rangle}{\partial y} = -\frac{A\alpha}{[(\Delta-1)\alpha^2]^{1/2}} \quad (19)$$

From the equation (19) it is required to calculate A(α) : Where $\alpha = a/(Dt)^{1/2}$

which describes the slopes of the dislocation tails, this will help us to obtain Δ which will help us to get the dislocation diffusion coefficient [6]. For this we have the next expression:

$$A^2(\alpha) = \frac{8}{\pi^2} \int_0^{\infty} \frac{e^{-z^2} dz}{z[J_0^2(z\alpha) + Y_0^2(z\alpha)]} \quad (20)$$

Where z is the Integration variable

This expression was integrated numerically, the lower limit was truncated in 0.00001 because Y, is asymptotic, this value was considered as a favorable minimum for the calculation, while for the calculation of the upper limit it was truncated in the value 27.29 because the preceding values tend to zero, the results values obtained are shown in table 7.

Table 7. D' coefficient of diffusion due to the dislocations.

	A(α)	Δ	D' (cm^2/s)	β
Line 1	3.0340231	1.168E+10	1.17E-04	5.61E+05
Line 2	2.9421767	1.749E+11	4.09E-03	5.50E+06
Line 3	2.9507068	1.098E+11	2.37E-03	3.59E+06
Line 4	3.0255087	1.952E+10	2.12E-04	9.02E+05
Line 5	2.957074	7.591E+10	1.55E-03	2.55E+06
Line 6	2.9595759	9.154E+10	1.82E-03	3.12E+06

When the density of dislocations is sufficiently small, the graphs of $\ln\langle c\rangle vs.y^2$ are exactly linear and Deff = D, otherwise it is not negligible when the second term is not negligible and the dislocation contributes significantly to the total of the average concentration (<c>), the ln <c> may not represent linear variation with y^2 therefore, a single effective diffusion coefficient can not necessarily be defined.

First linear domain.

To calculate the effective diffusion coefficient, by equation (1) the dislocation density must be minimal or at the time of exposure it must also be short, for ranges of ε / α between 0 and 1

$$D_{eff} = (4t\frac{\partial \ln<c>}{\partial y^2})^{-1} \quad (1)$$

Second linear domain

To calculate the effective diffusion coefficient, under the second linear domain the following characteristics must be fulfilled: High dislocation densities, sufficiently long exposure times and the relationship $\varepsilon/\alpha \geq 10$ which will allow us to calculate the diffusion coefficient by Hart expression equation (7). He pointed out that when ε / α is sufficiently large, so that the length exceeds sufficiently, there could be sampling by diffusion of atoms from many regions of dislocation and areas of the crystal sufficient to make it generally look Fickian and describable to a single D_{eff}. Hart estimated that the D_{ff} should tend towards the mean of D 'and D.

However, the theory finds that Deff does not differ by more than 30% from the value of $D_{Hart,}$, and therefore the second linear domain can be redefined as the range from infinity to the smallest for which the graphics Log <c> vs. y^2, its linearity is not experimentally distinguished and therefore it produces a unique D_{eff}. For this case it's finding the coefficient $\varepsilon/\alpha \geq 10$ so will be used to calculate the effective coefficient of Ni, second linear domain and is presented in table 8. So that the length exceeds sufficiently, there could be a sampling by diffusion of atoms from many regions of dislocation and regions of the crystal sufficient to make it generally look Fickian and describable to a single D_{eff} Hart estimated that the D_{ff} should tend towards the mean of D 'and D.

Table 8. Effective Diffusion Coefficient D_{Hart}.

	D_{Hart} (cm^2/s)	$(Dt)^{1/2}$ (cm)
Line 1	2.14E-12	1.04E-03
Line 2	7.43E-11	1.59E-03
Line 3	4.30E-11	1.53E-03
Line 4	3.85E-12	1.08E-03
Line 5	2.82E-11	1.49E-03
Line 6	3.31E-11	1.47E-03
Average	3.08E-11	1.38E-03

Table 9. Diffusion measurements of the Ni in polycrystals of UDIMET 500.

Metal	T range (°C)	d (cm^{-2})	$(Dt)^{1/2}$ (cm)	α
UDIMET 500	1050	d ~ 2.31E6	1.403×10^{-3}-1.47×10^{-3}	3.14×10^{-5} - $4.80\ 10^{-5}$

t =30,000h on service.

RESULTS AND DISCUSSION

Thermal barrier with 30,000 h approximately of service was analyzed and measured through the analysis in an SEM. With the variation of the composition of the Nickel in the analyzed zone and linear defects present. It was able to evaluate the effective diffusion coefficient, utilizing Smoluchowski modeling and boundary conditions proposed by A.D Le Claire and A. Rabinovitch. From the values obtained in six lines of the effective diffusion coefficient in the sample, a high atomic diffusion is observed, induced by the presence of edge defects in the analysis area. The movement of the Nickel in the superalloy causes the possible restructuring of the substrate in the area of analysis: the appearance of the Widmanstätten structure and changes in the composition of the coating with an increase in the chemical composition of Aluminum and Nickel. These elements are between the layer and the substrate. The presence of Fe and Mo which do not belong to the bond coat, as well as a decrease in the composition of the Cobalt (also belongs to the substrate), likewise it was observed. The elements of the Top Coat they spread to the Bond Coat because of concentrations of Zr in the Bond Coat area and an increase in the composition of the Yttrium. From these conclusions, we could consider that the zone is promising for the failure of the material at high temperatures and with a time of short service.

ACKNOWLEDGMENTS

The authors want to thank full to the LAPEM and the Guanajuato University for their support for this investigation.

Bibliography

[1] A.D. Le Claire and A. Rabinovitch J. Physics 1984, Volume C: Solid State Physics 17, 991. IOP Science pp. 260.

[2] Hart W.E Acta Metall (1957) 5, 597. On the role of dislocations in bulk diffusion. Acta Metall. 5:597. [General Electric Research Lab., Schenectady, NY] CC’’’’’’

[3] Reed R. C. The Superalloys: Fundamentals and Applications. Cambridge, Cambridge University Press, 2006. ISBN: 9780521859042. Cap. 2, pp.33-99

[4] Zlateva G., Martinova Zlatanka, Microstructure of Metals and Alloys an Atlas of Transmission Electron Microscopy Images, CRC Press Ed., USA. 2008, ISBN: 978- 1- 4200-7556-4. pp. 4-13

[5] Cullity B. D. Elements of X-Ray Diffraction Ed.1, USA 1956. Addison- Wesley Publishing Company Inc, p.125

[6] Murch G., Nowick A., Diffusion in Crystalline Solids, Academic Press Inc., USA, 1984. ISBN: 0-12-522662-4. p. 260-263

[7] Bose S.,High Temperature Coatings. Elsevier Inc. 2007. Linacre House, Jordan Hill. Oxford, UK. ISBN 13: 978-0-7506-8257-7